Received: 12 July 2022 | Revised: 19 September 2022 | Accepted: 24 September 2022

DOI: 10.1111/jace.18825

Journal of the American Ceramic Society

RESEARCH ARTICLE

Chipping of ceramic-based dental materials by micrometric particles

Estíbaliz Sánchez-González[1] | **Óscar Borrero-López**[1] | **Fernando Rodríguez-Rojas**[1] | **Mark Hoffman**[2] | **Fernando Guiberteau**[1]

[1]Departamento de Ingeniería Mecánica, Energética y de los Materiales, Universidad de Extremadura, Badajoz, Spain

[2]School of Engineering, University of Newcastle, Newcastle, Australia

Correspondence
Óscar Borrero-López, Departamento de Ingeniería Mecánica, Energética y de los Materiales, Universidad de Extremadura, 06006 Badajoz, Spain.
Email: oborlop@unex.es

Funding information
Ministry of Science and Innovation, Spain, Grant/Award Number: PID2019-105377RB-I00; Junta de Extremadura, Spain; FEDER/ERDF, Grant/Award Number: GR18149

Abstract

Chipping caused by micrometric particles poses a threat to the structural integrity of modern dental prosthetic materials. It can degrade their fracture strength and cause wear of both artificial crowns and antagonist teeth. Here, surface chipping of the main types of commercial ceramic-based dental materials at the microcontact/particle level is investigated by means of indentation tests. Conical tips of different sizes (radii 20 and 200 μm) under axial and sliding loading are employed to simulate individual microcontacts. Both decreasing particle size and adding a lateral contact force decrease the chipping load below typical bite forces. Specific damage mechanisms are identified as predominantly brittle fracture in ceramics with small, equiaxed crystals, with significant quasi-plastic damage in ceramics containing large, elongated crystals and composites. Critical loads for the occurrence of chipping are quantified (lowest values in equiaxed glass–ceramics; greatest in zirconia) and analyzed within the framework of fracture mechanics. The brittleness index (*BI*) is proposed as a simple indicator of the resistance to chipping of dental materials—the lower the *BI*, the greater the resistance. Special attention is paid to the effect of the materials' microstructure, which can result in transformation toughening (as in zirconia) or quasi-plastic behavior (as in lithium disilicate), both highly beneficial to increasing the chipping resistance. Finally, practical implications for the selection of current dental materials as well as for the development of novel materials with improved durability are discussed.

KEYWORDS

brittleness, chipping, dental ceramics, durability, microstructure, quasi-plasticity

1 | INTRODUCTION

Chipping refers to the wholesale dislodgement of relatively large fragments of material (chips) due to fracture caused by concentrated stresses from contact against a spurious sharp object. It poses a major threat to the structural integrity of engineering ceramics and other brittle materials.[1–4]

One field where chipping is particularly relevant is dentistry, as many of the commercial materials currently employed in dental prostheses are ceramic, or ceramic-based, and are therefore inherently brittle.[5–13] As opposed

to wear, which occurs gradually due to cyclic contacts, tooth chipping typically takes place as a result of a bite overload in a single event, when the fracture strength of the crown material is exceeded. Owing to relatively low fracture toughness, macroscopic, median cracks originating on the contact (occlusal) surface of a dental prosthesis propagate until they reach the sidewalls of the tooth, thereby leading to the formation of relatively large (i.e., macro) chips.[1] This is termed edge chipping, and in the dental context, it can result in catastrophic failure when the size of the chip is large enough.[14] Natural enamel provides greater resistance to chipping than artificial materials as the propagation of such cracks is hindered due to its *R*-curve behavior[15–17] but is not immune.[6,18]

Critically, particles are often present in the oral cavity, originating from both external (e.g., extrinsic silica-based atmospheric dust) and internal (e.g., intrinsic opaline phytoliths in plant food, fragments of dislodged tooth material) sources. Such particles typically have sizes of between one and hundreds of μm[19,20] and can be highly deleterious to tooth durability. Indeed, although particles are not necessarily harder than the crown material, they often contain sharp edges that greatly intensify the contact stress field.[21,22] The local damage that they produce, even at low (subthreshold) loads, decreases the strength of the material[23] and accelerates the long-term mechanical degradation in the form of wear.[20,24–26]

One phenomenon that has been less studied in dental materials is the occurrence of chipping damage induced by sharp, micrometric particles, that is, not macroscopic chipping events from tooth–tooth contacts but rather chipping at the microcontact/particle level. Although such small-scale events would not be immediately catastrophic because the size of the chip is micrometric, they pose a threat to the structural integrity by degrading the fracture strength to a significantly greater extent than subthreshold microcontacts.[23] Dislodged chips containing sharp edges can in turn cause secondary chipping and wear. Furthermore, the attendant increase in surface roughness is likely to result in a very aggressive wear of the opposing dentition (antagonist wear).[27–29]

The previous warrants detailed investigation of the chipping caused by particles in commercially available dental ceramics. Particle sizes between tens and hundreds of μm are considered, which are representative of both extrinsic and intrinsic grits.[19,20] This work focuses on surface chipping and looks at effects of both loading and particle/material aspects. The phenomenon is simulated by means of indentation tests with conical tips. First, critical chipping loads arising from axial and sliding contacts with particles/tips of different sizes are determined and analyzed using indentation fracture mechanics. The effects of material microstructure (monolithic vs. composite) are then established. A distinction is made between materials showing a "classic" brittle response and materials somewhat more resistant to chipping due to a quasi-plastic response. The results and analyses presented are expected to provide useful insights for the selection of currently available dental materials, as well as guidelines to improve the durability of novel materials.

2 | EXPERIMENTAL PROCEDURES

The materials investigated were obtained from commercially available CAD/CAM (computer-aided design/computer-aided manufacturing) blocks, heat-treated in dedicated dental furnaces (VITA ZYRCOMAT 6000 MS, VITA Zahnfabrik H. Rauter GmbH & Co. KG, Germany; and Multimat Touch, Dentsply, PA, USA) in a dental/prosthetic facility (Clínica Dental David Maestre, Valverde de Leganés, and LAB Dental, Badajoz, Spain), following the manufacturer's requirements.

Commercial, pre-sintered zirconia (Z) blocks (VITA YZ Translucent Zirconia, VITA Zahnfabrik H. Rauter GmbH & Co. KG, Germany) were fully densified by initial heating to 950°C at 10°C/min, followed by heating to 1500°C at 6°C/min, soaking for 90 min, and natural cooling to room temperature by shutting the furnace power off. The whole cycle was conducted pressureless in an air atmosphere.

Two lithium-containing glass–ceramics were crystallized in a vacuum atmosphere. A lithium disilicate (LD) material (IPS e.max CAD HT, Ivoclar Vivadent, NY, USA) was initially heated to 400°C (soaking 6 min), followed by heating to 820°C at 90°C/min (soaking 10 min), and heating to 840°C at 30°C/min (soaking 7 min); cooling was conducted gradually with the chamber closed until 550°C and then opening the furnace doors. A zirconia-reinforced lithium silicate (ZLS) material (Celtra Duo HT, Dentsply Sirona, NC, USA) was initially heated to 500°C (soaking 3 min), followed by heating to 820°C at 60°C/min (soaking 1 min), and gradual cooling with the chamber closed until 500°C, and then opening the furnace doors.

Feldspathic ceramic (F) (Vitablocs Mark II, VITA Zahnfabrik H. Rauter GmbH & Co. KG, Germany) and feldspathic ceramic–polymer composite (E) (VITA Enamic, VITA Zahnfabrik H. Rauter GmbH & Co. KG, Germany) materials were employed as received in dense CAD/CAM blocks.

When possible, human enamel (T) was used as control. In particular, specimens obtained from occlusal surfaces of unerupted molars donated by young adults were employed, after approval from the Bioethics Committee of the University of Extremadura (permit number 213//2019). Samples were preserved in refrigerated, fully hydrated environment until the moment of testing. In addition,

common soda–lime glass (G) was used to identify effects of the unique microstructure of human enamel.[30,31]

Plane parallel test specimens were obtained from all materials by mechanical cutting. Subsequently, the test surfaces of all specimens were gently ground with fine sandpaper, lapped (30 μm), and polished with diamond suspensions using routine ceramographic methods. The polishing routine consisted of the following steps: 15 μm (10 min), 9 μm (10 min), 6 μm (10 min), 3 μm (15 min), and 1 μm (20 min).

The microstructure of the materials was observed by scanning electron microscopy (FE-SEM; Quanta 3D FEG, FEI, the Netherlands) using secondary and backscattered electrons at intermediate accelerating voltages (10–15 kV). Specimens were not gold-coated prior to SEM examination. Zirconia was thermally etched at 1300°C in air to reveal grain boundaries.

Mechanical property characterization was undertaken by conventional indentation tests at room temperature in air. Vickers tests were performed with a diamond tip (MV-1, Matsuzawa, Japan). The maximum load applied was 9.8 N. A total of 10 indentations per material were performed. Hardness (H) and fracture toughness (K_{IC}) were determined from the dimensions of the indentation scars, as measured by optical microscopy (Epiphot 300, Nikon, Tokyo, Japan) and image analysis software, using standard formulae.[32,33] Hertzian tests were conducted (5535, Instron, Canton, MA, USA) on select specimens using loads (P) in between 15 and 3500 N, applied by WC spheres of different radii ($r = 4.76$–1.58 mm), following procedures described elsewhere to construct Hertzian indentation stress ($P_0 = P/\pi a^2$)–strain (a/r) curves, where a is the contact radius measured by optical microscopy.[34]

High-performance indentation tests were used to investigate chipping. Tests were conducted at room temperature in air, using dedicated, computer-controlled equipment (Revetest RST3, Anton Paar, Graz, Austria), which can apply a maximum load of 200 N. Rockwell-C indenters of different radii (200 and 20 μm) were employed, which simulate contacts with micrometric particles of different sizes. Tests in both axial and sliding loading (scratch) configurations were conducted on polished surfaces. Because chipping takes place upon unloading,[1] the critical chipping load, defined as the lowest indentation load that causes chipping, cannot be determined from the load–displacement curve in a single indentation test.[35] Alternatively, comprehensive series of tests at different loads were conducted. Specifically, in the axial tests, for each material and tip size, separate pretests were performed at 50 N/min, progressively increasing maximum load. The initial loading intervals between tests were relatively large (20 N). The test surfaces were subsequently inspected by optical microscopy to determine the load intervals within which chipping had taken place first. Such intervals were subsequently scanned in more detail/resolution, using smaller loading steps (between 1 and 5 N). Every test/load was repeated three times. Surfaces were again inspected by optical microscopy after testing to accurately determine critical chipping loads. Because stochasticity influences the occurrence of chipping to some extent,[1] a uniform criterion needs to be established. In particular, the critical chipping load was considered to be the smallest load for which all three of the three indentations at such load showed a well-formed chip particle. Tests were also conducted in sliding mode. In particular, for each material and tip size, three sliding tests (sliding speed 5 mm/min) at progressively increasing normal load from an initial value of 1 N (loading rate 100 N/min with the large tip; 25 N/min with the small tip), resulting in scratches of length 5 mm, were performed.[a] Test surfaces were subsequently examined by optical microscopy. For each scratch, critical chipping load was calculated from the corresponding microscopy image using the sliding speed and loading rate.[36,37] The surface of select chipped off specimens after testing was inspected in greater detail by optical microscopy and SEM.

3 | RESULTS

Figure 1 shows the microstructure of the materials investigated. Such microstructures have been analyzed in detail elsewhere.[38–41] Briefly, dental zirconia (Z, Figure 1A) shows a polycrystalline microstructure, with grains of submicrometric size. Although tetragonal zirconia is the majority phase in order to achieve greater toughness, dental zirconia typically also contains some proportion of cubic phase (~30%) to improve translucency.[38]

LD (Figure 1B), ZLS (Figure 1C), and feldspathic ceramic (F, Figure 1D) are all glass–ceramics consisting of ceramic crystal particles embedded in a silicate glass–matrix.[39,42] In LD and F, crystals are relatively large, with sizes between μm (LD) and tens of μm (F) units. Crystals are elongated in LD (aspect ratio over 4) and equiaxed in F. ZLS also contains elongated crystals (aspect ratio 3.5), but of smaller size (by a factor 3) than LD, together with nanometric, equiaxed crystals, and its matrix is zirconosilicate glass.[41] Enamic (E, Figure 1E) is a versatile composite variant of F, consisting of a continuous network of open feldspathic ceramic infiltrated by a polymeric resin.[40]

[a] Enamel could not be tested in sliding configuration because the size of flat, polished surfaces that can be obtained on the occlusal surface of human teeth without removing the outer enamel layer are too small to fit in scratches under the same loading conditions as those employed in the artificial materials.

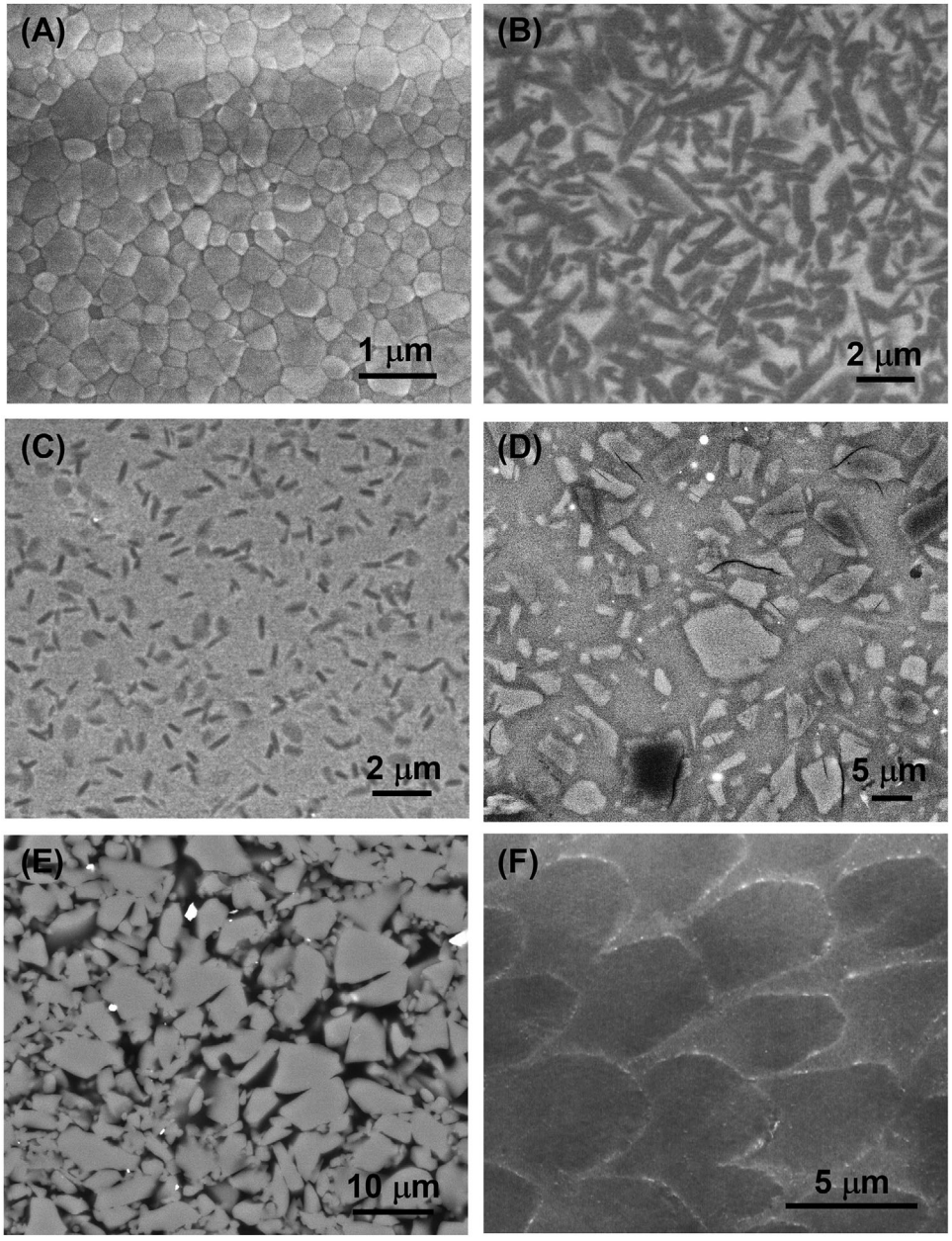

FIGURE 1 Scanning electron microscopy (SEM) images representative of the microstructure of the dental materials used in this study: (A) zirconia; (B) lithium disilicate; (C) zirconia-reinforced lithium silicate; (D) feldspathic ceramic; (E) Enamic (ceramic–polymer composite); and (F) human dental enamel (occlusal surface).

For comparison, the microstructure at the occlusal surface of natural tooth enamel (T) is shown in Figure 1F. Human enamel is a hierarchical bio-composite.[17,31] Its structural units at the microstructural scale are elongated, mineral (hydroxyapatite) rods of near-circular section (diameter ≈ 5 μm). The rods are tightly packed, oriented perpendicular to the occlusal surface, and are separated by less mineralized sheaths. The rod–sheath interfaces are relatively weak.[30]

Table 1 lists the mechanical properties of the materials. All of them except Enamic are harder than natural enamel. Zirconia is a factor of 3 harder than enamel and about a factor of 2 harder than the glass–ceramics. Among the latter group, ZLS is slightly harder than LD and F. Zirconia is also significantly tougher than the other dental materials, with LD and E following but at considerable distance. The rest of the glass–ceramics have K_{IC} values comparable to that of natural enamel.

Figure 2 shows optical micrographs representative of the surface chipping damage under axial loading up to 200 N. For relatively large contacts (r = 200 μm), simulating coarse grit, the response of the materials can be

TABLE 1 Mechanical properties (modulus, E; hardness, H; fracture toughness, K_{IC}) and brittleness index (BI) of the dental materials employed in this study.

Material	Modulus, E (GPa)	Hardness, H (GPa)	Toughness, K_{IC} (MPa·m$^{1/2}$)	Brittleness index, $BI \times 10^3$ (m$^{-1/2}$)
Zirconia (Z)	210[a]	11.9 ± 0.1	6.1 ± 0.4	1.93
Lithium disilicate (LD)	88.3[b]	5.6 ± 0.1	1.20 ± 0.05	4.67
Zirconia-lith.sil. (ZLS)	99.2[b]	6.2 ± 0.2	0.87 ± 0.05	7.13
Feldspathic ceramic (F)	48[a]	5.2 ± 0.6	0.9 ± 0.2	5.53
Enamic (E)	30[a]	3.3 ± 0.3	1.33 ± 0.09	2.48
Tooth enamel (T)	70[a]	4.0 ± 0.3	0.7 ± 0.1	5.71
Soda–lime glass (G)	72.5[c]	5.2 ± 0.1	0.67 ± 0.05	7.76

[a]From Ref. [38].
[b]Measured from Hertzian indentation tests (Figure S5).
[c]From Ref. [22]

classified into two groups. On the one hand, two of the glass–ceramics (ZLS, Figure 2E; and F) show a characteristically brittle behavior, with large, well-formed surface chips originated after contact at moderate loads, which are well within regular bite forces.[43] On the other hand, the other glass–ceramic (LD, Figure 2C), the ceramic–polymer composite (E), and zirconia (Figure 2A) have not undergone chipping by the end of the tests. Their response is akin to that of a more plastic material, with deformation dominating over catastrophic fracture. Non-catastrophic fracture in the form of radial cracks is observed, which is indicative of a quasi-plastic, rather than plastic (i.e., dislocation-controlled), response.[44] It is noted that, compared to the glass–ceramics, the extent of radial cracking is significantly decreased in zirconia, tending closer to classic plastic behavior.[45]

For relatively small axial contacts ($r = 20$ μm), simulating fine grit, all the materials undergo chipping, including those immune to it under larger contacts (Z, Figure 2B; LD, Figure 2D; and E). The chipping loads observed with the smaller tip are in all cases lower than those found with the larger tip (Table S1). However, the size of the chips is considerably smaller than that obtained with the larger tip. Comparatively, chips in zirconia are significantly smaller than in the other materials.

As control, chipping tests were also conducted on human enamel and glass, as shown in Figure 2G,H. Indeed, it can be observed that despite having the same mechanical property values, the responses of enamel and glass are fundamentally different. Although glass shows clear brittle behavior with extensive cracking/chipping from relatively low loads with both large and small particles, the enamel evidences a mostly plastic/quasi-plastic response dominated by deformation, only showing stable radial cracks at high loads (no chipping).

Figure 3A–E shows images representative of the damage induced by relatively large sliding contacts ($r = 200$ μm), at progressively increasing load. As with axial contacts, the response of the materials can be classified into predominantly brittle and ductile/quasi-plastic. The former group includes ZLS (Figure 3B), F, and E. They all display initial plastic deformation at relatively low loads, followed by stable fracture in the form of partial cone cracks perpendicular to the sliding direction at intermediate loads, and eventually radial cracks and chipping at greater loads (visible at lower magnifications), much like in conventional glass (Figure 3C). Higher magnification details of partial cone cracks and radial cracks are shown in parts (D) and (E) of Figure 3, respectively. Abundant debris of relatively large size is also observed in the vicinity of the scratch tracks. The latter group includes Z and LD (Figure 3A). In those materials, the transition from deformation to fracture/chipping takes place at greater loads, and the size of the chips and number of pieces of debris are comparatively smaller than in the more brittle materials.

Figure 3F,G shows images representative of the scratch tracks produced by sliding contacts with smaller particles ($r = 20$ μm). Now, the damage transitions directly from initial plastic deformation into radial cracking and chipping, without prior partial cone cracks. In that sense, the response of all materials under the smaller contact shifts toward being somewhat less brittle, with the debris of significantly smaller size than those produced by larger particles. As with axial contacts, decreasing particle size results in a decrease in the critical load at which chipping is first observed in all materials. Moreover, the chipping loads observed under sliding contact were in all cases lower than the critical loads obtained from axial contact with the same particles (Table S1).

Figure 4 shows SEM images representative of the chipping damage from both axial and sliding contact in select materials (ZLS, F, and LD). In all cases, the occurrence of chipping is accompanied by a large increase

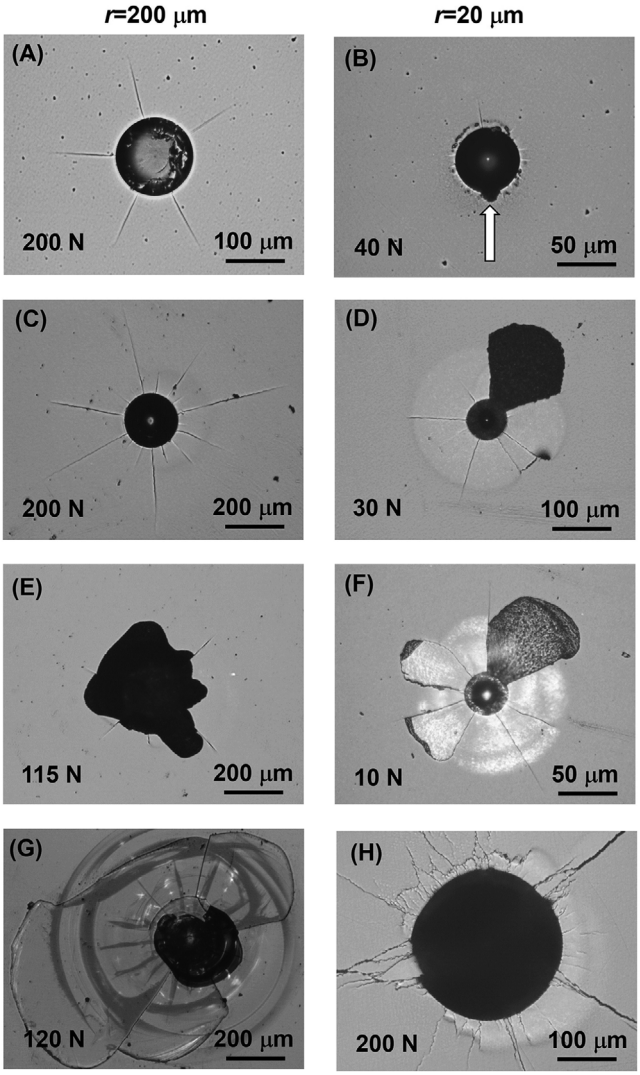

FIGURE 2 Select optical micrographs after indentation tests in axial mode using Rockwell-C tips of radii 200 μm (left column) and 20 μm (right column). In each case, the maximum applied load is indicated in the lower left corner of the image: (A) and (B) zirconia; (C) and (D) lithium disilicate; (E) and (F) zirconia-reinforced lithium silicate; (G) soda–lime glass; and (H) human dental enamel (occlusal surface). Images for all the materials investigated are provided in Figures S1 and S2.

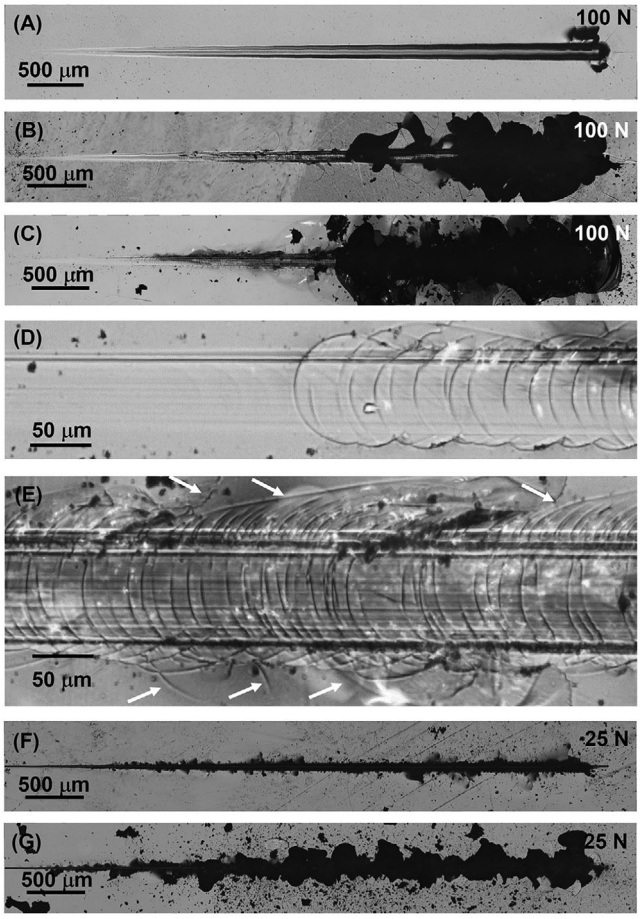

FIGURE 3 Select optical micrographs (panoramic view) after indentation tests in sliding mode. In each case, the maximum applied normal load is indicated in the upper right corner of the image: (A) lithium disilicate, $r = 200$ μm; (B) zirconia-reinforced lithium silicate, $r = 200$ μm; (C)–(E) soda–lime glass, $r = 200$ μm, with white arrows pointing at radial cracks; (F) lithium disilicate, $r = 20$ μm; (G) zirconia-reinforced lithium silicate, $r = 20$ μm. Images for all the materials investigated are provided in Figures S3 and S4.

in the surface roughness compared with the polished surrounding regions. Higher magnification details of the surface in chipped off regions (Figure 4C,D) reveal abundant, strength-degrading cracks and microcracks, as well as the loose particle debris of micrometric and submicrometric size displaying sharp edges. The fracture mode is generally mixed. Transgranular fracture is predominant across glassy phases (Figure 4E) and crystals/grains of larger size.[44,46] Increasing the crystal aspect ratio and content effectively shift the fracture mode to intergranular, as revealed by cleavage steps conforming to crystal contours. This is evidenced, for example, in LD (Figure 4F) compared with ZLS (Figure 4E). The toughening resulting from intergranular fracture[33,44] leads to spall particles of smaller size and is thus highly beneficial to resist chipping.

4 | DISCUSSION

We have shown how indentation tests can be adapted to simulate chipping of dental materials at the micro-contact/particle level. Particles of micrometric size are ubiquitous in the oral cavity, both from external (extrinsic grit) and internal (intrinsic grit) sources. All commercial dental materials investigated—zirconia, glass–ceramics and composites—underwent chipping at relatively

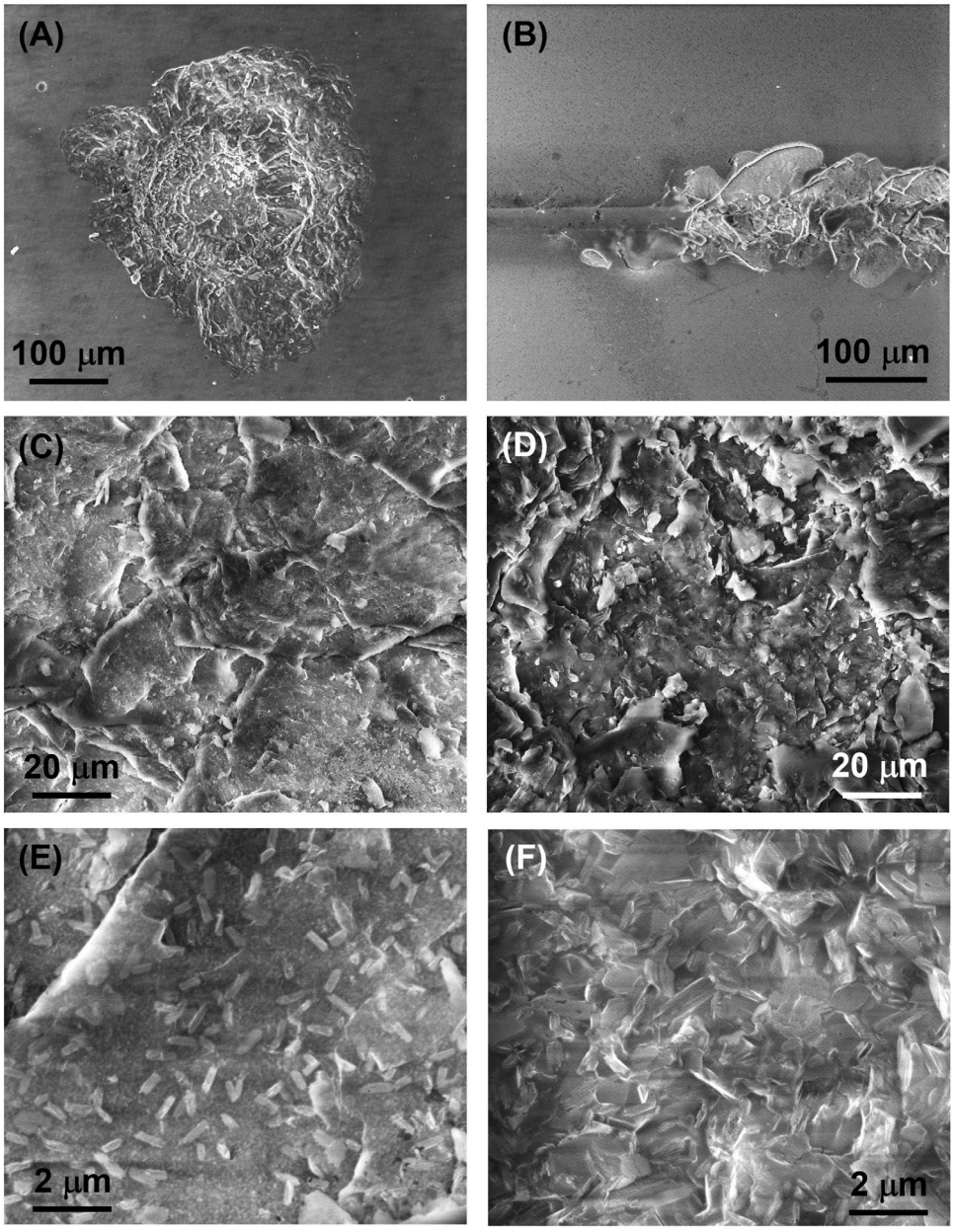

FIGURE 4 Scanning electron microscopy (SEM) images representative of the microscopic damage after chipping tests in select dental materials: (A) low-magnification image of a chipping site in feldspathic ceramic after axial loading with a Rockwell-C tip of radius 20 μm; (B) low-magnification image of a chipping site in zirconia-reinforced lithium silicate after sliding loading with a tip of radius 20 μm. Parts (C) and (D) are intermediate-magnification images of a chipping site in zirconia-reinforced lithium silicate and feldspathic ceramic, respectively. Parts (E) and (F) are high-magnification images of a chipping site in zirconia-reinforced lithium silicate, and lithium disilicate, respectively.

modest loads in laboratory tests. Such loads are well within the range of regular bite forces in humans.[43]

4.1 | Mechanics

The mechanics of chipping have been reviewed recently by Lawn.[1] Surface chipping from a concentrated axial load is depicted schematically in Figure 5A. It is a result of the extension of subsurface lateral cracks (initial size c_0) from the plastic zone during unloading, driven by residual stresses originated by the elastic–plastic mismatch. The wear particle/chip is finalized upon the attraction of the lateral cracks (final size c_f) to the free surface. Smaller chips spanning only a near-circular arc can form by the coalescence of lateral and radial cracks, as seen, for example, in Figure 2D. The exposed fracture surface reveals the details of crack propagation, with intergranular fracture being more effective than transgranular fracture at achieving greater impedance/toughness. A fracture mechanics

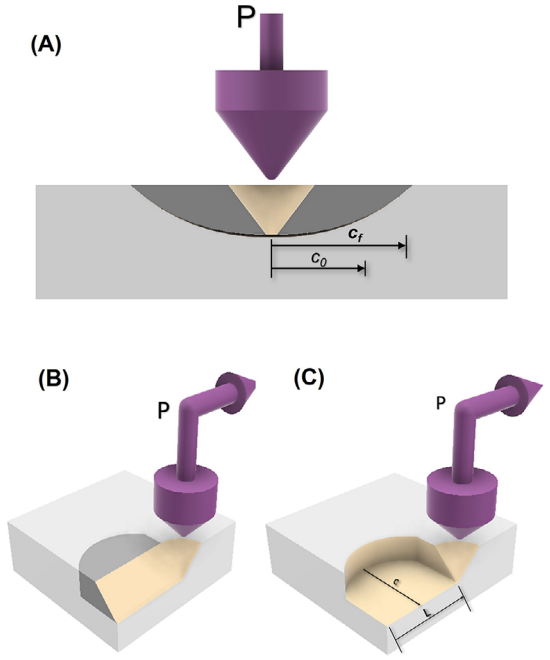

FIGURE 5 Schematics of chipping processes from concentrated loads (P) in brittle materials: (A) surface chipping from axial loading; and (B) and (C) surface chipping from sliding contact, where c is the length of the lateral crack, and L the sliding distance. In parts (A) and (B), regions in cream color represent the penetration of the indenter, and regions in dark gray indicate the volume engulfed by the chip particle. In part (C), the region in cream color represents the wear scar left by removal of the chip particle.

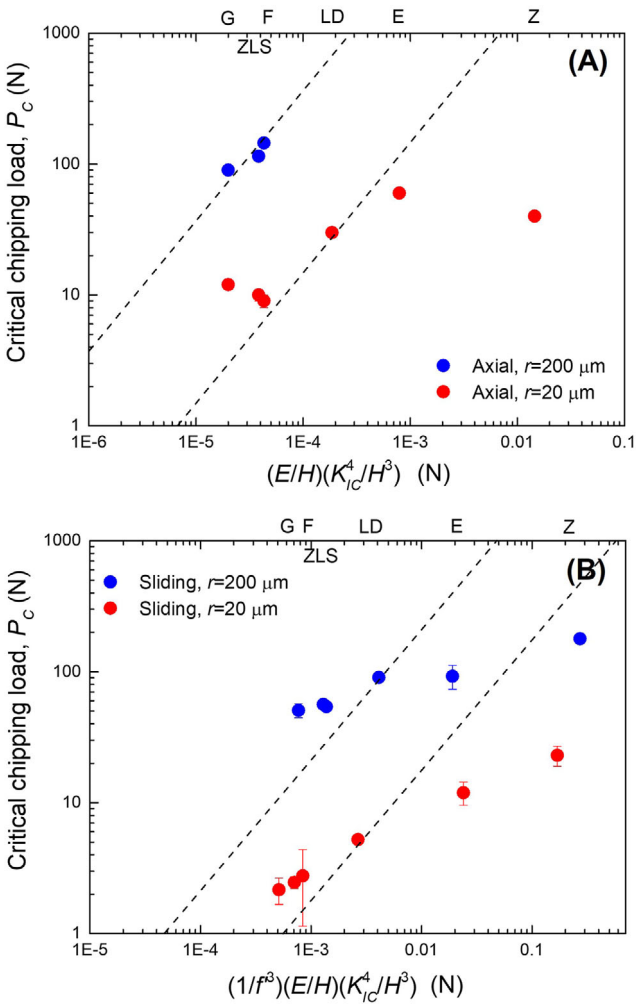

FIGURE 6 Log–log plots of (A) critical chipping load, P_C, from indentation tests in axial contact versus $(E/H)(K_{IC}{}^4/H^3)$; and (B) critical chipping load, P_C, from indentation tests in sliding contact versus $(1/f'^3)$ $(E/H)(K_{IC}{}^4/H^3)$. Symbols on the top x-axis indicate the different dental materials: Z (zirconia), E (Enamic), LD (lithium disilicate), F (feldspathic ceramic), ZLS (zirconia-reinforced lithium silicate), and G (glass). Dashed lines correspond to lines of slope 1 on the log–log plots (fracture mechanics prediction).

analysis of lateral crack extension in a brittle solid results in the following expression for the critical chipping load, P_C:

$$P_{C,\,axial} = \alpha \left(\frac{E}{H}\right)\left(\frac{K_{IC}^4}{H^3}\right) \qquad (1)$$

where α is a dimensionless coefficient, and the term (E/H) accounts for the effect of the residual stress field.

Equation (1) predicts slope 1 in a log–log plot of $P_{C,\,axial}$ versus $(\frac{E}{H})(\frac{K_{IC}^4}{H^3})$. Such a plot is shown in Figure 6A using the experimental P_C values. Although the fit is far from perfect, Equation (1) nevertheless roughly captures the general trends of the experimental data. Zirconia is a notable outlier, deviating from the fracture mechanics prediction to a greater extent likely due to its transformation toughening behavior, which makes it closer to a ductile material.[45]

For sliding contacts, the mechanism of chip formation differs from that of axial contact and is depicted schematically in Figure 5B,C.[21,23,47] In a sliding contact, the extension of lateral cracks is assisted by friction-induced, relatively large tensile stresses at the rear of the moving contact. The maximum tensile stress is given by[48]:

$$\sigma_{max} = P_0 \left(\frac{1-2\nu}{3} + \frac{4+\nu}{8} f\right) = P_0\, f' \qquad (2)$$

where P_0 is the contact pressure, and f' is an effective coefficient of friction (CoF) that compounds the actual CoF (f) and the material's Poisson ratio (ν).

The tensile stress below the surface is proportional to σ_{max}.[34,48] Lateral crack extension is expected to initiate from larger flaws there when that stress equals the fracture strength. Considering that H scales with P_0, and

combining Equation (2) with fundamental indentation fracture mechanics [33,44] leads to:

$$P_{C,\,sliding} = \frac{\beta}{f'3}\left(\frac{E}{H}\right)\left(\frac{K_{IC}^4}{H^3}\right) \quad (3)$$

where β is a dimensionless coefficient.

Equation (3) is a modified version of Equation (1) for sliding contacts, which includes the CoF. It is qualitatively consistent with the experimental results in the sense that it predicts a shift toward lower values of critical loads in sliding contacts compared to axial-only by increasing friction. Figure 6B shows a log–log plot of $P_{C,sliding}$ versus $\frac{1}{f'3}(\frac{E}{H})(\frac{K_{IC}^4}{H^3})$. Like Equation (1), Equation (3) only roughly captures the general trends of the experimental P_C data, and the fit again leaves room for improvement, with zirconia, the most prominent outlier.

Given the relatively complex dependency of Equations (1) and (3) on material properties and the CoF, a simpler, empirical alternative to correlate P_C with material properties is considered. Because chipping is predominantly a brittle process, and based on the analytical expressions of Equations (1) and (3), it is hypothesized that a correlation exists between the chipping load and the brittleness index (*BI*). The *BI* is defined as the ratio between hardness and fracture toughness[49] and is a straightforward measure of the competition between deformation- (lower *BI*) and fracture-dominated (greater *BI*) mechanical behavior.

Figure 7 shows plots of critical chipping loads versus *BI* (calculated from H and K_{IC} values, Table 1). Indeed, critical loads appear to follow a linear correlation with *BI* in all four groups: large and small particles, axial and sliding contacts. The Pearson correlation coefficients (R) of least-square linear fits are 0.99 (large particles, axial), 0.90[a,b] (large particles, sliding), 0.88 (small particles, axial), and 0.88[a] (small particles, sliding). The *BI* is thus proposed as a simple indicator of the susceptibility of dental materials to undergoing surface chipping: The lower the *BI*, the greater the critical load/chipping resistance. Figure 7 permits a clear visualization of the effects of both loading and particle size on chipping. For all materials, sliding contacts result in lower chipping loads than axial-only contacts, due to the additional frictional forces. Likewise, decreasing particle size results in lower chipping loads due to increased contact pressure.

[b] Transformation-toughened zirconia was excluded from the fit.

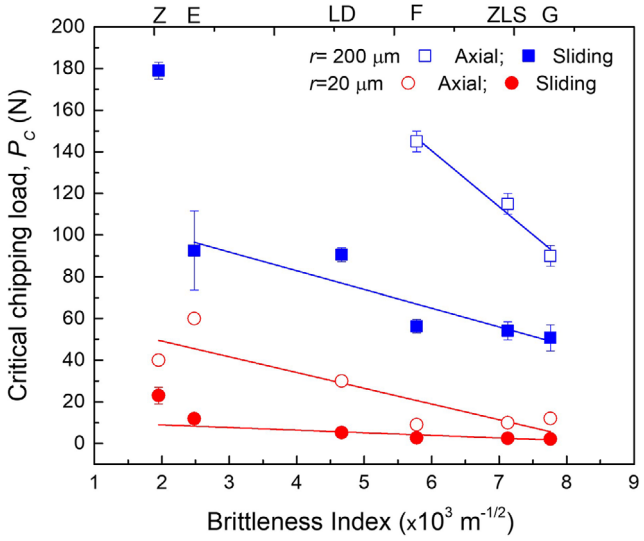

FIGURE 7 Critical chipping load, P_C, from indentation tests in axial and sliding contacts with Rockwell-C tips of radius 200 μm and 20 μm versus brittleness index. Symbols on the top *x*-axis indicate the different dental materials: Z (zirconia), E (Enamic), LD (lithium disilicate), F (feldspathic ceramic), ZLS (zirconia-reinforced lithium silicate), and G (glass). Solid lines correspond to least-square fits to each set of data.

4.2 | Effects of the materials' microstructure

The microstructures of the synthetic dental materials investigated in this study can be classified into two basic groups: monolithic (zirconia) and composite (the rest). In general, monolithic ceramics tend to be more brittle than composites, as microstructural toughening mechanisms behind the tip such as crack bridging are less effective.[33,44] Zirconia is a notable exception, because the tetragonal→monoclinic phase transformation and attendant change in volume enables considerable toughening ahead of the crack tip.[45] Phase transformation toughening in zirconia in fact results in its having the lowest *BI* of all the materials considered. In turn, this makes zirconia the most resistant to chipping of all the dental materials (Figure 7).

Ceramic-based dental composites are typically regarded as being less strong and wear-resistant than monoliths.[39] The key microstructural feature in composite materials is the presence of weak interphases, which generally result in quasi-plastic mechanical behavior. Increasing a material's quasi-plasticity results in a lower *BI* and, thus, increases its resistance to chipping. This is because interfacial cracking dissipates stress and hinders the initiation of other cracks, for example, lateral cracks, while accompanying toughening mechanisms behind the crack tip impede propagation.

The degree of quasi-plasticity depends on the specific material microstructure. It is typically enhanced by increasing the fraction of reinforcement/matrix interphases and the size of such reinforcements. An illustrative example is the comparison between the LD (Figure 1B) and ZLS (Figure 1C) materials. They are both lithium-based glass–ceramics and have similar chemical composition, with microstructures based on reinforcing crystals embedded in a glass–matrix. But LD contains significantly larger and more elongated crystals than ZLS, which confer on it enhanced ductility (lower H) and a greater K_{IC}, and thus a lower *BI*. Moreover, the presence of zirconium in the glassy phase of ZLS results in a more brittle matrix, which also contributes to its lesser extent of quasi-plasticity and greater *BI*. Note that a fully glassy material (e.g., conventional soda–lime glass) results in extremely brittle behavior, with extensive cracking (Figures 2G and 3C–E) and chipping at low loads.

The mechanical differences between LD and ZLS are further demonstrated in Figure S5, obtained from the Hertzian indentation tests. Enhanced quasi-plasticity in LD results in a stress–strain curve with a significantly larger degree of nonlinearity compared with ZLS (Figure S5A). The more brittle behavior of ZLS results in its damage mode being dominated by cone cracks originated during loading (Figure S5B), whereas in LD, a transition to radial cracks (originated during unloading) takes place at relatively large contact pressures (Figure S5C,D), typical of quasi-plastic materials.[34,44]

Finally, it is important to mention that the only material immune to surface chipping from axial contacts is the natural enamel (Figure 2H). Interestingly, the enamel has basically the same single-value mechanical properties as glass, which in contrast shows an extremely brittle behavior and very low chipping loads. The main difference between the two materials is their microstructure: amorphous, uniform in glass, and hierarchical bio-composite in enamel.[17,31] Somewhat paradoxically, the resistance to chipping of the enamel stems from its built-in structural weakness: Damage is easily generated at rod/sheath interfaces but is prevented from coalescing and reaching the surface by the highly anisotropic disposition of mineral rods.[30,50] The resilience of enamel is thus a result of its ability to tolerate, rather than suppress, damage.[51]

4.3 | Practical implications

Laboratory indentation tests demonstrate that all modern ceramic-based dental materials can undergo chipping from concentrated loads upon regular chewing. In the oral cavity, such concentrated loads can be delivered by micrometric particles containing sharp edges. Although chipping at the microcontact/particle level does not result in immediate catastrophic failure, it can degrade fracture strength [23] and cause secondary chipping and wear. Because chipping increases the surface roughness, it can also accelerate the wear of the opposing dentition.[27–29]

Selection of durable dental materials should therefore take chipping into account. The *BI* provides a simple indicator of materials' resistance to chipping. In principle, materials with relatively low *BI* require greater loads to chip (and can also form smaller chips). However, as usual with materials selection, trade-offs of the properties involved should be taken into account. For example, except for zirconia, low *BI* materials are relatively soft and thus prone to faster mechanical degradation in the form of wear. That is the case of ceramic–polymer composites and LD, which also have relatively poor fracture strength.[38] Zirconia is the strongest and has the lowest *BI* of all the dental materials but achieves it by means of its greater fracture toughness, remaining significantly harder than natural enamel (by over a factor of 3). Consequently, it can accelerate wear of antagonist teeth unless the contact surface is very smooth. Moreover, zirconia is less machinable and possesses poorer aesthetics compared with the other dental materials and is susceptible to degradation at low temperature (ageing).[52,53]

Particle size and loading configurations also affect chipping significantly. Both decreasing particle size and increasing friction result in chipping at lower loads. Implications for chewing mechanics and diet should be considered accordingly. For example, diets based on items that could contain intrinsic grit (e.g., opaline phytoliths in plant foods), or foods which have not been properly processed and contain even small residues of dust/sand/crust (e.g., shellfish) could result in a greater tendency to chipping, especially when lateral chewing forces are required.

As per the design of novel dental materials with improved resistance to chipping, the general guideline is to engineer the microstructure to aim for a low *BI*, keeping property trade-offs in mind. Of the currently available dental materials, perhaps monolithic zirconia offers the best prospects. Due to its baseline low *BI*, the resistance to chipping of zirconia is already significantly better than that of the other dental materials. Further improvements could be achieved by adjusting its phase composition and employing processing additives that can reduce its hardness—while simultaneously improving translucency and protecting from low-temperature degradation.[52,54,55] Alternatively, tailoring two-phase microstructures to further enhance quasi-plasticity also has the potential to improve chipping resistance. This requires relatively large reinforcing crystals and relatively weak crystal–matrix interfaces, which effectively shift the strategy for durability to damage containment. It should be noted that, of all the materials considered in this study, only the natural enamel was immune to surface chipping from both small and large

axial contacts under the load interval investigated (up to 200 N). This suggests the biomimetic design of novel composites as an attractive strategy for the development of dental materials with improved durability.[31,40,56]

5 | CONCLUSIONS

We have employed indentation tests with micrometric tips to investigate surface chipping at the microcontact/particle level in commercial, ceramic-based dental materials. Based on the results and analyzes, the following conclusions can be drawn:

1. Indentation tests can be adapted to simulate chipping of dental materials at the microcontact/particle level.
2. Ceramic-based dental materials undergo chipping from concentrated loads by micrometric particles at loads well within regular bite forces.
3. For particles of fixed geometry and size, sliding contacts result in chipping at lower loads than axial contacts because of frictional forces.
4. Within the micrometric range, decreasing particle size results in chipping at lower loads due to increased contact pressure.
5. The brittleness index (*BI*) offers a simple measure of the resistance to chipping of dental materials under both axial and sliding contacts: The lower the *BI*, the greater the resistance.
6. Chipping is ultimately controlled by the material's microstructure: transformation-toughened, monolithic materials; and quasi-plastic two-phase, composite materials with relatively large crystals, are the most resistant to chipping. Glass-dominated materials result in brittle behavior and relatively low chipping resistance.

ACKNOWLEDGMENTS

Inspiring discussions with Brian Lawn are gratefully acknowledged. This study was supported by the Ministry of Science and Innovation, Spain (Grant Number: PID2019-105377RB-I00), and the Junta de Extremadura, Spain and FEDER/ERDF funds (Grant Number: GR18149).

REFERENCES

1. Lawn BR. Chipping: a pervasive presence in nature, science and technology. J Mater Sci. 2021;56(14):8396–405.
2. Chai H, Lawn BR. A universal relation for edge chipping from sharp contacts in brittle materials: a simple means of toughness evaluation. Acta Mater. 2007;55(7):2555–61.
3. Chai H, Lawn BR. Edge chipping of brittle materials: effect of side-wall inclination and loading angle. Int J Fract. 2007;145(2):159–65.
4. Lawn BR, Swain MV, Phillips K. Mode of chipping fracture in brittle solids. J Mater Sci. 1975;10(7):1236–9.
5. Brandeburski SBN, Vidal ML, Collares K, Zhang Y, Bona AD. Edge chipping test in dentistry: a comprehensive review. Dent Mater. 2020;36(3):E74–84.
6. Chai H, Lee JJW, Lawn BR. On the chipping and splitting of teeth. J Mech Behav Biomed Mater. 2011;4(3):315–21.
7. Quinn GD, Giuseppetti AA, Hoffman KH. Chipping fracture resistance of dental CAD/CAM restorative materials: Part 2. Phenomenological model and the effect of indenter type. Dent Mater. 2014;30(5):E112–23.
8. Quinn GD, Giuseppetti AA, Hoffman KH. Chipping fracture resistance of dental CAD/CAM restorative materials: Part I – Procedures and results. Dent Mater. 2014;30(5):E99–111.
9. Swain MV. Unstable cracking (chipping) of veneering porcelain on all-ceramic dental crowns and fixed partial dentures. Acta Biomater. 2009;5(5):1668–77.
10. Zhang Y, Chai H, Lee JJW, Lawn BR. Chipping resistance of graded zirconia ceramics for dental crowns. J Dent Res. 2012;91(3):311–5.
11. Zhang Y, Lee JJW, Srikanth R, Lawn BR. Edge chipping and flexural resistance of monolithic ceramics. Dent Mater. 2013;29(12):1201–8.
12. Argyrou R, Thompson GA, Cho SH, Berzins DW. Edge chipping resistance and flexural strength of polymer infiltrated ceramic network and resin nanoceramic restorative materials. J Prosthet Dent. 2016;116(3):397–403.
13. Pfeilschifter M, Preis V, Behr M, Rosentritt M. Edge strength of CAD/CAM materials. J Dent. 2018;74:95–100.
14. Rekow D, Thompson VP. Engineering long term clinical success of advanced ceramic prostheses. J Mater Sci Mater Med. 2007;18(1):47–56.
15. Bajaj D, Arola DD. On the R-curve behavior of human tooth enamel. Biomaterials. 2009;30(23–24):4037–46.
16. Bajaj D, Park S, Quinn GD, Arola D. Fracture processes and mechanisms of crack growth resistance in human enamel. JOM. 2010;62(7):76–82.
17. Wilmers J, Bargmann S. Nature's design solutions in dental enamel: uniting high strength and extreme damage resistance. Acta Biomater. 2020;107:1–24.
18. Constantino PJ, Lee JJW, Chai H, Zipfel B, Ziscovici C, Lawn BR, et al. Tooth chipping can reveal the diet and bite forces of fossil hominins. Biol Lett. 2010;6(6):826–9.
19. World Health Organization. Occupational and Environmental Health Team . Hazard prevention and control in the work environment: airborne dust. Geneva, Switzerland: World Health Organization; 1999.
20. Rodriguez-Rojas F, Borrero-Lopez O, Constantino PJ, Henry AG, Lawn BR. Phytoliths can cause tooth wear. J R Soc Interface. 2020;17(172), https://doi.org/10.1098/rsif.2020.0613
21. Hutchings I, Shipway P. Tribology: friction and wear of engineering materials. 2nd ed. Oxford UK: Butterworth-Heinemann; 2017; ISBN-10: 0081009100; ISBN-13: 978-0081009109.
22. Constantino PJ, Borrero-Lopez O, Pajares A, Lawn BR. Simulation of enamel wear for reconstruction of diet and feeding behavior in fossil animals: a micromechanics approach. Bioessays. 2016;38(1):89–99.

23. Lawn BR, Huang H, Lu M, Borrero-Lopez O, Zhang Y. Threshold damage mechanisms in brittle solids and their impact on advanced technologies. Acta Mater. 2022;232:117921.
24. Borrero-Lopez O, Pajares A, Constantino PJ, Lawn BR. A model for predicting wear rates in tooth enamel. J Mech Behav Biomed Mater. 2014;37:226–34.
25. Borrero-Lopez O, Pajares A, Constantino PJ, Lawn BR. Mechanics of microwear traces in tooth enamel. Acta Biomater. 2015;14:146–53.
26. Borrero-Lopez O, Constantino PJ, Lawn BR. Role of particulate concentration in tooth wear. J Mech Behav Biomed Mater. 2018;80:77–80.
27. Mitov G, Heintze SD, Walz S, Woll K, Muecklich F, Pospiech P. Wear behavior of dental Y-TZP ceramic against natural enamel after different finishing procedures. Dent Mater. 2012;28(8):909–18.
28. Santos F, Branco A, Polido M, Serro AP, Figueiredo-Pina CG. Comparative study of the wear of the pair human teeth/Vita Enamic (R) vs commonly used dental ceramics through chewing simulation. J Mech Behav Biomed Mater. 2018;88:251–60.
29. Preis V, Behr M, Handel G, Schneider-Feyrer S, Hahnel S, Rosentritt M. Wear performance of dental ceramics after grinding and polishing treatments. J Mech Behav Biomed Mater. 2012;10:13–22.
30. Borrero-Lopez O, Constantino PJ, Bush MB, Lawn BR. On the vital role of enamel prism interfaces and graded properties in human tooth survival. Biol Lett. 2020;16(8), https://doi.org/10.1098/rsbl.2020.0498
31. Thompson VP. The tooth: an analogue for biomimetic materials design and processing. Dent Mater. 2020;36(1):25–42.
32. Anstis GR, Chantikul P, Lawn BR, Marshall DB. A critical-evaluation of indentation techniques for measuring fracture-toughness. 1. Direct crack measurements. J Am Ceram Soc. 1981;64(9):533–8.
33. Green DJ. An introduction to the mechanical properties of ceramics. Cambridge, UK: Cambridge University Press; 1998.
34. Lawn BR. Indentation of ceramics with spheres: a century after Hertz. J Am Ceram Soc. 1998;81(8):1977–94.
35. Borrero-Lopez O, Hoffman M, Bendavid A, Martin PJ. A simple nanoindentation-based methodology to assess the strength of brittle thin films. Acta Mater. 2008;56(7):1633–41.
36. Borrero-Lopez O, Hoffman M. Measurement of fracture strength in brittle thin films. Surf Coat Technol. 2014;254:1–10.
37. Borrero-Lopez O, Hoffman M. Sliding-contact fracture of brittle layers. In: Zhang S, editor. Thin films and coatings: toughening and toughness characterization (advances in materials science and engineering). Boca Raton, FL: CRC Press; 2015. p. 529–85.
38. Borrero-Lopez O, Guiberteau F, Zhang Y, Lawn BR. Wear of ceramic-based dental materials. J Mech Behav Biomed Mater. 2019;92:144–51.
39. Borrero-Lopez O, Guiberteau F, Zhang Y, Lawn BR. Inverse correlations between wear and mechanical properties in biphasic dental materials with ceramic constituents. J Mech Behav Biomed Mater. 2020;105:103722.
40. Martinez-Vazquez FJ, Sanchez-Gonzalez E, Borrero-Lopez O, Miranda P, Pajares A, Guiberteau F. Novel bioinspired composites fabricated by robocasting for dental applications. Ceram Int. 2021;47(15):21343–9.
41. Rodríguez-Rojas F, Borrero-López O, Sánchez-González E, Hoffman M, Guiberteau F. On the durability of zirconia-reinforced lithium silicate and lithium disilicate dental ceramics. Wear. 2022;508:204460.
42. Lubauer J, Belli R, Peterlik H, Hurle K, Lohbauer U. Grasping the lithium hype: insights into modern dental lithium silicate glass-ceramics. Dent Mater. 2022;38(2):318–32.
43. Lee JJW, Constantino PJ, Lucas PW, Lawn BR. Fracture in teeth-a diagnostic for inferring bite force and tooth function. Biol Rev. 2011;86(4):959–74.
44. Lawn BR. Fracture of brittle solids. Cambridge, UK: Cambridge University Press; 1993.
45. Garvie RC, Hannink RH, Pascoe RT. Ceramic steel. Nature. 1975;258(5537):703–4.
46. Borrero-Lopez O, Ortiz AL, Gledhill AD, Guiberteau F, Mroz T, Goldman LM, et al. Microstructural effects on the sliding wear of transparent magnesium-aluminate spinel. J Eur Ceram Soc. 2012;32(12):3143–9.
47. Evans AG, Marshall DB. Wear mechanisms in ceramics. In: Fundamentals of friction and wear of materials. Metals Park, OH: American Society of Metals; 1980.
48. Hamilton GM, Goodman LE. Stress field created by a circular sliding contact. J Appl Mech. 1966;33(2):371.
49. Lawn BR, Marshall DB. Hardness, toughness, and brittleness – indentation analysis. J Am Ceram Soc. 1979;62(7–8):347–50.
50. Sánchez-González E, Rodríguez-Rojas F, Pinilla-Cienfuegos E, Borrero-López O, Ortiz AL, Guiberteau F. Bioinspired design of triboceramics: learning from the anisotropic micro-fracture response of dental enamel under sliding contact. Ceram Int. 2020;16(18):27983–9.
51. Borrero-Lopez O, Rodriguez-Rojas F, Constantino PJ, Lawn BR. Fundamental mechanics of tooth fracture and wear: implications for humans and other primates. Interface Focus. 2021;11(5), https://doi.org/10.1098/rsfs.2020.0070
52. Zhang Y, Lawn BR. Novel zirconia materials in dentistry. J Dent Res. 2018;97(2):140–7.
53. Chevalier J. What future for zirconia as a biomaterial? Biomaterials. 2006;27(4):535–43.
54. Turon-Vinas M, Roa JJ, Marro FG, Anglada M. Mechanical properties of 12Ce-ZrO2/3Y-ZrO_2 composites. Ceram Int. 2015;41(10):14988–97.
55. Kohorst P, Borchers L, Strempel J, Stiesch M, Hassel T, Bach FW, et al. Low-temperature degradation of different zirconia ceramics for dental applications. Acta Biomater. 2012;8(3):1213–20.
56. Wegst UGK, Bai H, Saiz E, Tomsia AP, Ritchie RO. Bioinspired structural materials. Nat Mater. 2015;14(1):23–36.

SUPPORTING INFORMATION

Additional supporting information can be found online in the Supporting Information section at the end of this article.

How to cite this article: Sánchez-González E, Borrero-López Ó, Rodríguez-Rojas F, Hoffman M, Guiberteau F. Chipping of ceramic-based dental materials by micrometric particles. J Am Ceram Soc. 2023;106:1309–1320. https://doi.org/10.1111/jace.18825